JOURNAL OF MATERIALS SCIENCE 30 (1995) 3515–3520

Influence of calcination temperature on the properties of spray dried alumina–zirconia composite powders

M. BALASUBRAMANIAN, S. K. MALHOTRA* AND C. V. GOKULARATHNAM
*Department of Metallurgical Engineering, *FRP Research Centre, Indian Institute of Technology, Madras 600036, India*

Alumina–zirconia composite powders containing 10, 12.5, 15 or 20 wt % zirconia were prepared by spray-drying the hydroxide gels. These powders were calcined at 650 and 950 °C. The spray-dried as well as the calcined powders were characterized by means of Coulter counter, Sorptometer, infrared spectroscopy (i.r.), scanning electron microscopy (SEM), thermogravimetric analysis (TGA) and X-ray diffraction (XRD). Initially the spray-dried powders are amorphous and spherical in shape with a diameter of 6 μm and crystallize after calcination treatment at 950 °C. Sintered density of the 950 °C calcined powder compacts was higher than 650 °C calcined powder compacts. Compacts made from 650 °C treated powders retained 100% tetragonal phase after sintering irrespective of composition. Some amount of tetragonal phase is transformed into monoclinic phase in the composites containing higher amount of zirconia in the sintered compacts made from 950 °C calcined powders.

1. Introduction

A clever use of martensitic transformation in ZrO_2 to toughen ceramic matrices is an active area of research [1–3]. The transformation of tetragonal ZrO_2 (t-ZrO_2) to the monoclinic ZrO_2 (m-ZrO_2) involves an anisotropic volume increase (more than 3%) and shear strain (about 6%), which is the factor that increases the toughness by various mechanisms [4]. Thus it is important to retain the tetragonal form until the component is going into service.

This can be achieved by the introduction of stabilizing agents [5], strain [6] or surface free energy factors [7, 8]. When considering the Al_2O_3 matrix, the last two are important factors. The strain is due to the higher modulus of Al_2O_3 matrix (370 GPa) compared to that of the t-ZrO_2 (200 GPa). The surface energy depends on the size [9] and shape [10] of the dispersed ZrO_2 particles which are critically influenced by the processing methodology. Homogeneous as well as fine dispersions of ZrO_2 particles in the Al_2O_3 matrix can be obtained by chemical mixing of the constituents in solution state or in sol state. Zircoaluminates [11], alkoxides [12] or chlorides [9] have been used as the starting materials to prepare Al_2O_3–ZrO_2 powders. The chemically derived powders are either amorphous [11] or crystalline [13] depending on the processing conditions. Calcination of this powder leads to the evolution of volatiles and phase changes [11]. Retention of t-ZrO_2 and densification was also influenced by the calcination of powders [14]. ZrO_2 content [15, 16] and its distribution [6], (i.e. whether it is present within Al_2O_3 grains or grain boundaries) has a profound influence on the retention of t-ZrO_2.

In the present work a study has been made to assess the influence of calcination temperatures on the properties of spray-dried Al_2O_3–ZrO_2 composite powders prepared from aluminium sulphate and zirconium oxychloride. The effect of ZrO_2 content on the retention of t-ZrO_2 was also studied.

2. Experimental procedures

The detailed procedures involved in the preparation of composite powder are reported in [17]. In this study the same procedure was followed with some modifications. Reagent grade aluminium sulphate and zirconium oxychloride were mixed in required proportions so that the resulting composites contained 10.0, 12.5, 15.0 or 20.0 wt % of ZrO_2. The salts were dissolved in double distilled water and heated to 90 °C. The sol formation at pH 4 was performed by the addition of ammonium hydroxide with vigorous stirring. It was converted into gel at pH 9 by further addition of ammonium hydroxide by pouring the required amount in a single addition. The resulting gel was filtered and washed thoroughly with dilute ammonia followed by distilled water to remove the precipitation by-products to a minimum level. After filtering it was dispersed in water and the pH was maintained at 6 by the addition of nitric acid. This slurry was spray-dried at 210 °C in a mini spray drier (Buchi 190). The powder was further dried at 110 °C (termed AS hereafter) in an oven to remove residual moisture and then calcined at 650 (CAL6) or 950 °C (CAL9) for 5 h.

0022–2461

Particle size analysis and BET surface area determination of the dried and calcined powders have been carried out by a Coulter counter and nitrogen adsorption (Sorptomatic Series 1800) respectively. The powder morphology was studied by scanning electron microscopy (Jeol JSM 5400). Thermogravimetric analysis (Stanton Redcroft STA-780) was performed on the AS sample at a heating rate of 5 °C min^{-1} up to 1200 °C. The powders were dispersed in KBr pellets and the i.r. absorption was measured in the range 4000–400 cm^{-1} (Shimadzu model 470). All the above characterization was done for the powders containing 15 wt % ZrO_2.

The calcined powders were pressed by uniaxial single action press into cylindrical pellets by applying a pressure of 200 MPa. Green densities were calculated by measuring the compact dimensions and weight. These pellets were then sintered for 3 h at 1650 °C. Density of the sintered specimen was determined by Archimedes method using water as the immersion medium. Theoretical densities of these compositions were calculated and the green and sintered densities are reported relative to these density values. Phases present in the powders and sintered samples have been determined by X-ray diffraction (Philips PW 1710) using CoK_α radiation with an iron filter. The XRD patterns obtained from the as-sintered surface were used to calculate the percentage of t-ZrO_2 in each specimen using the equation given below [18]

$$\% \text{ t-}ZrO_2 = \frac{I_t(1\,1\,1)}{I_m(1\,1\,\bar{1}) + I_m(1\,1\,1) + I_t(1\,1\,1)} \times 100 \quad (1)$$

where $I(hkl)$ is the intensity of diffracted beam from the particular (hkl) plane, m is the monoclinic phase and t is the tetragonal phase.

3. Results

The average particle size of the spray-dried powder found by the Coulter counter is 6 μm (Fig. 1) which is also confirmed by SEM (Fig. 2). This particle size is lower than that obtained in the previous study [17]. This is probably due to the lower pH of the gel used for spray drying. Coulter counter analysis also reveals a narrow particle size distribution and a slight increase in average particle size due to calcination. Fig. 3 shows the morphology of the powders observed by SEM. The particles are spherical in shape, looking like a cotton ball. It appears that the powders are aggregates of loosely packed fine particles. The specific surface area and specific pore volume of powders are given in Table I. The initial powder has a very low surface area and pore volume; it is somewhat higher for the CAL9 powders and even higher for the CAL6 powders.

XRD patterns of the powders (Fig. 4) show that these are amorphous up to 5 h calcining at 650 °C and crystalline phases started forming after calcining at 950 °C. TGA of the spray-dried powder is shown in Fig. 5. This also reveals that the formation of oxides occur above 900 °C since there was a large amount of

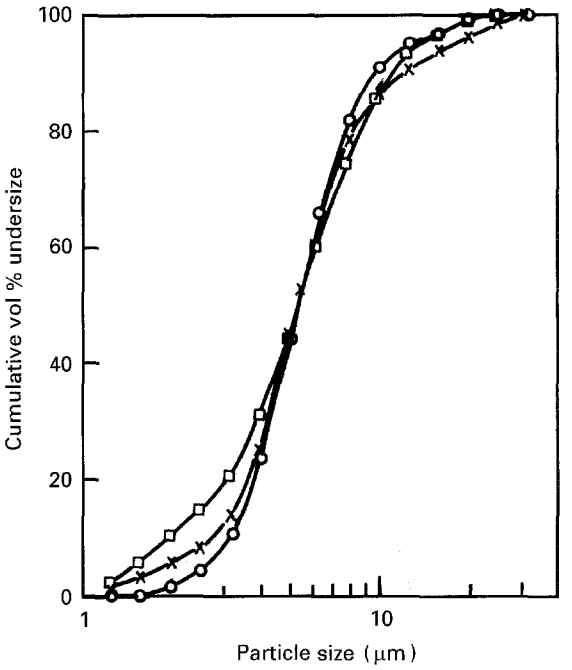

Figure 1 Coulter counter analysis of particle size distribution. ○ AS – spray dried powder; □ CAL6 – Calcined at 650 °C; × CAL9 – Calcined at 950 °C.

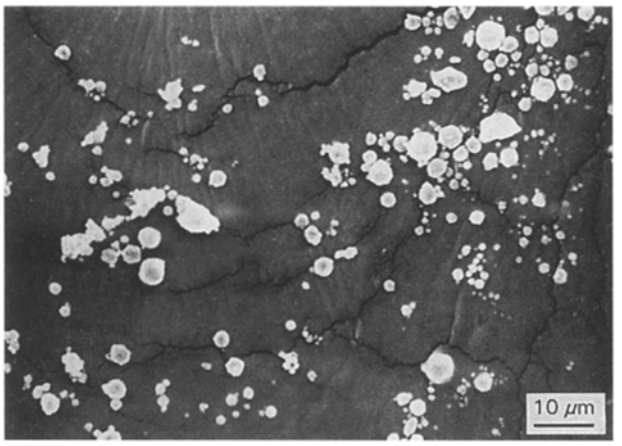

Figure 2 SEM micrograph of the spray-dried powder.

weight loss at this temperature due to the evolution of hydrates. The free water molecules and hydroxyl groups have characteristic vibration frequencies which absorb energy in the i.r. region. Boehmite doublets are expected at 3280 cm^{-1} and 3080 cm^{-1} corresponding to the stretching mode of Al–O–H and at 1145 cm^{-1} and 1073 cm^{-1} corresponding to Al–O–H bending mode. The broad bands at 950 and 650 cm^{-1} are attributed to the presence of pseudoboehmite and the intense absorption due to the O–H bending band at 1060 cm^{-1} and the broad band centred around 720 cm^{-1} for intermediate boehmite. Normally the absorption bands of pseudoboehmite are covered by the stretching vibration of an adhesive water molecule [19]. The adhesive water is identified by the absorptions at 3500 cm^{-1} (O–H stretching vibrations) and 1630 cm^{-1} (O–H bending vibrations). The broad band in the region 1000–400 cm^{-1} corresponds to Al–O vibrational modes [20]. Fig. 6 shows the i.r. absorption spectra of the spray-dried and calcined

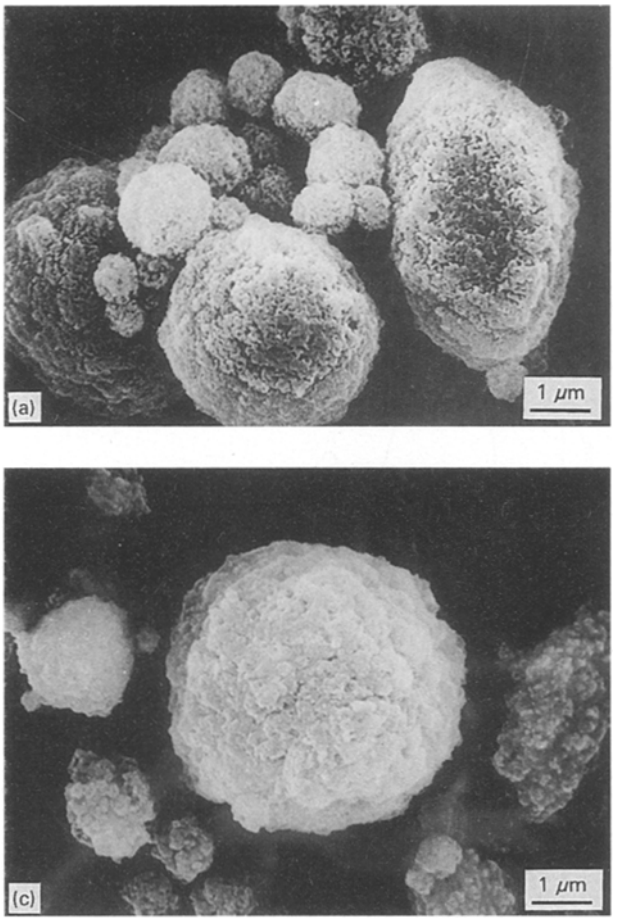

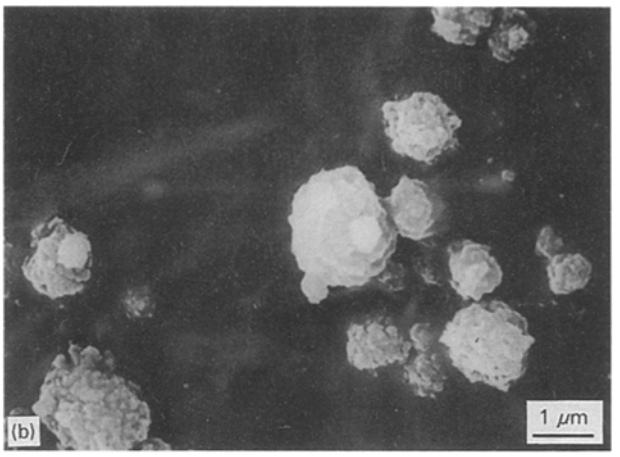

Figure 3 SEM micrograph of spray-dried and calcined powders. (a) Spray dried powder; (b) Calcined at 650 °C; (c) Calcined at 950 °C.

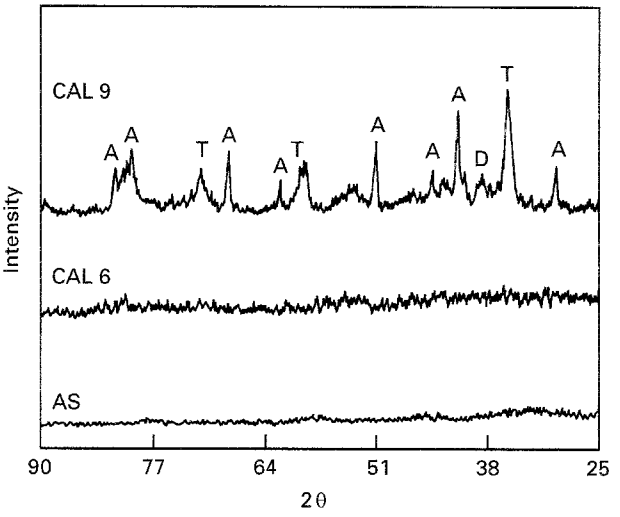

Figure 4 XRD patterns of the spray-dried and calcined powders. A, α-Al_2O_3; T, t-ZrO_2; D, δ-Al_2O_3.

TABLE I Specific surface area and specific pore volume of spray-dried and calcined powders

	BET surface area ($m^2 g^{-1}$)	Specific pore volume ($cm^3 g^{-1}$)
As-sprayed	6.92	3.96×10^{-3}
Calcined at 650 °C	57.94	27.40×10^{-3}
Calcined at 950 °C	20.32	8.96×10^{-3}

powders. The spray-dried powder contain bands corresponding to free water, boehmite and pseudoboehmite. After calcination at 650 °C the characteristic doublets corresponding to boehmite and the band corresponding to pseudoboehmite partially disappeared, but the O–H vibrations of adhesive water were still present. The 950 °C treatment leads to the conversion of all hydroxides into oxides, as is evident from the disappearance of Al–OH vibrations. The band corresponding to the α-Al_2O_3 has started forming. Even this treatment did not lead to the full elimination of water. In the spray-dried powder a band appeared at 1400 cm^{-1} which corresponds to the HNO_3 molecule [21]. This band has been shifted to 1380 cm^{-1} after calcination which corresponds to the $Al(NO_3)_3$ molecule. But the peak corresponding to this compound is not observed in the XRD patterns of the calcined powders.

XRD patterns of the sintered samples derived from the CAL6 powders are shown in Fig. 7. It reveals that the phases present in the 10 wt % ZrO_2 samples are α-Al_2O_3 and t-ZrO_2 whereas traces of m-ZrO_2 are also present in the samples containing 12.5 wt % ZrO_2 and above. Fig. 8 shows the XRD pattern of the CAL9 derived samples. In this case 100% t-ZrO_2 is retained in the samples containing 10 wt % ZrO_2 and trace amounts of m-ZrO_2 are present in the 12.5 and 15 wt % ZrO_2 samples. About 49% of the t-ZrO_2 is transformed in the samples containing 20 wt % ZrO_2.

The values of green density, sintered density and the weight loss after sintering of the compacts are given in Table II. The packing behaviour of particles as revealed by green density of the CAL6 powders is poorer than the CAL9 powders. The bulk density is only about 35% of the theoretical density for CAL6 powder compacts but it is > 40% for the CAL9 powders. Due to the presence of higher amounts of hydrates, weight loss after sintering is more for the CAL6 powder compacts than the CAL9 powder compacts. Sintered density of the CAL9 powder derived samples are found to be higher than the CAL6 powder derived compacts.

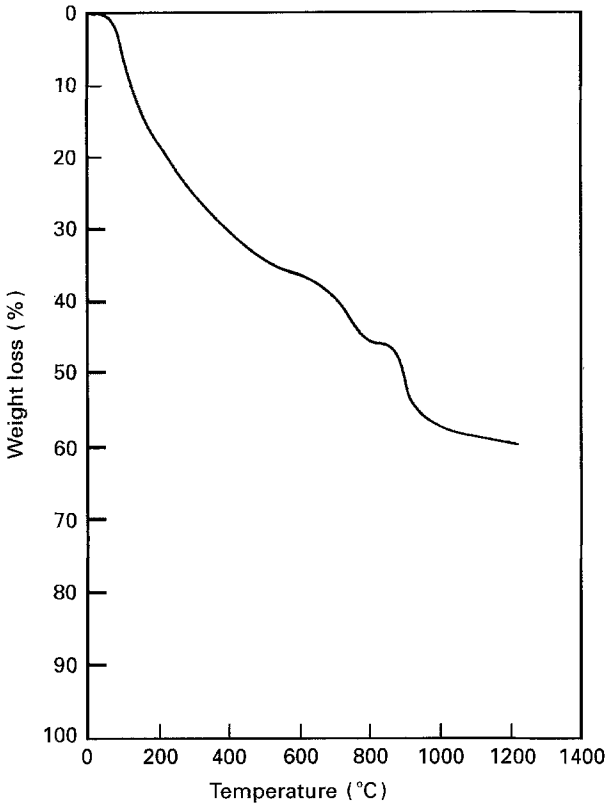

Figure 5 TGA thermogram of spray-dried powder.

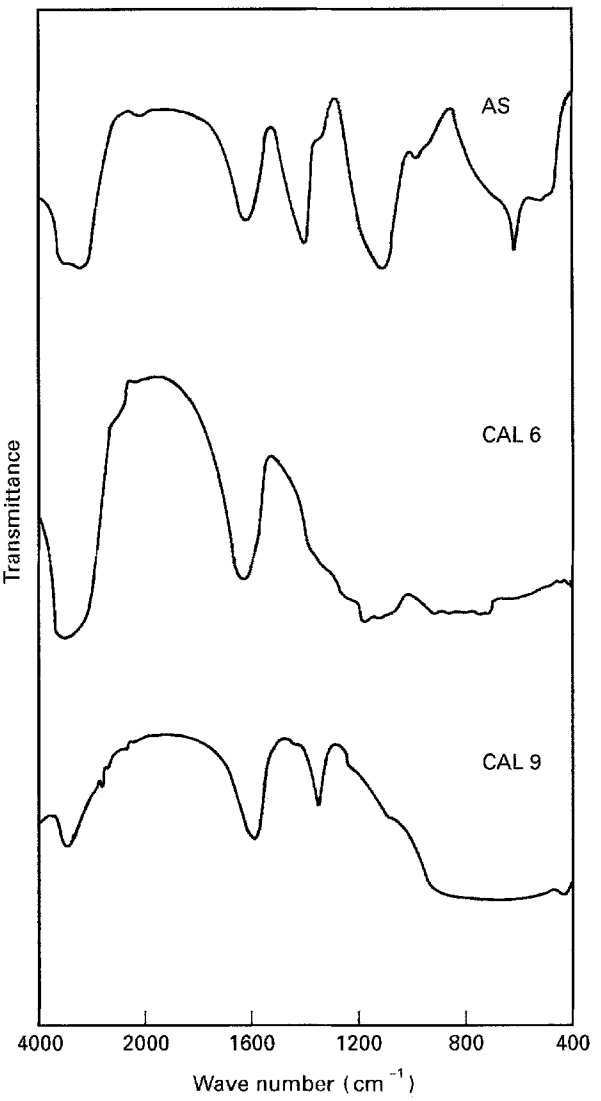

Figure 6 Infrared spectrum of the spray-dried and calcined powders. AS – Spray dried powder; CAL6 – Calcined at 650 °C; CAL9 – Calcined at 950 °C.

4. Discussion

Infrared spectra of the spray-dried powder shows that it is highly hydrated with the absorption at 3500 cm^{-1} and 1697 cm^{-1} corresponding to the free as well as the adsorbed water. Even after calcining at 950 °C it retains some amount of hydrates. During spray drying only the surface hydrates are removed by evaporation, which is also revealed by SEM micrograph (Fig. 3a). Since the hydrated surface is inaccessible to nitrogen used for surface area measurements, the specific surface area value should be very low [22]. It was observed that the hydroxides have a low surface area and pore volume. When it was heated just below the temperature at which the formation of low temperature Al_2O_3 starts, the adsorption isotherm showed that pores were formed [23]. Therefore it is expected that after 650 °C treatment a further amount of hydrates are removed, without any sintering. So the pores are open and more surface is available for nitrogen adsorption. It was also observed [23] that a drastic change occurs in the shape of the adsorption isotherm after heating at a much higher temperature. In that study the BET surface area was found to be half of its highest value and the calculations of the surface area and pore volume from the adsorption isotherms showed that the micro-pore volume decreased to a low value. So the powders started crystallizing and sintering after 950 °C treatment which leads to the closure of fine pores (Fig. 3c). This causes the observed surface area to decrease to one-third of its highest value. XRD pattern of the CAL9 powder (Fig. 4) clearly shows the presence of crystallites. Sharp peaks of t-ZrO_2 and broad peaks of δ-Al_2O_3 and α-Al_2O_3 appeared in this XRD pattern.

Earlier studies [24] suggested that the hydroxides are responsible for the tetragonal to monoclinic transformation during calcination. Small amounts of bound OH groups stabilised the tetragonal form at room temperature. When the solid was heated to about 600–900°C, the OH groups were driven off as water, and simultaneously the formation of monoclinic phase was noted. Here about 60% of hydrates are present in the spray-dried powder but it does not lead to the formation of monoclinic phase after the calcination. This rules out the possibility of the influence of hydroxyl groups on the transformation, so the factor controlling the stability of tetragonal form is the size of tetragonal crystallites. Based on the relations between surface area and particle size [25]

$$D = \frac{6}{\rho S} \tag{2}$$

where D is the particle diameter in microns, ρ is the density of the tetragonal phase in $g\,cm^{-3}$ and S is the BET surface area in $m^2\,g^{-1}$ it was found that the particle size of ZrO_2 is nearly 0.5 μm even assuming the particle size of Al_2O_3 and ZrO_2 to be equal. (Normally the ZrO_2 particle size will be lower, since it

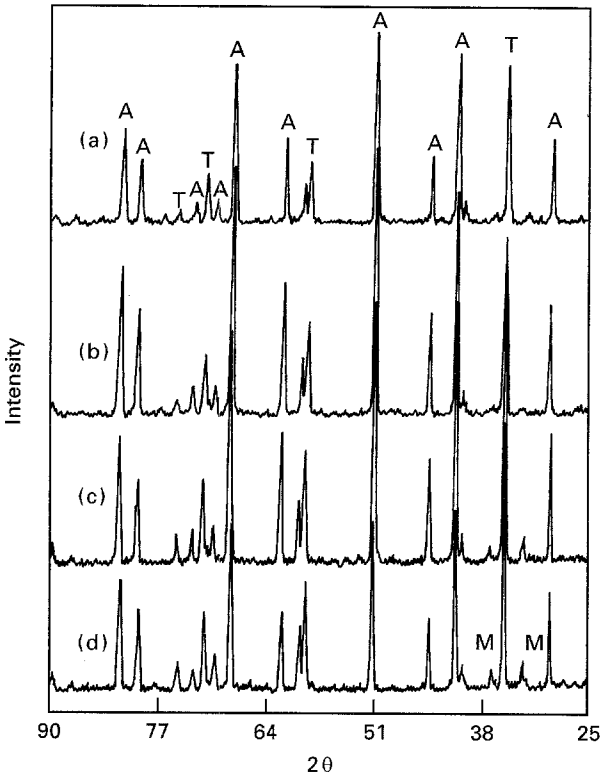

Figure 7 XRD patterns of the CAL6 powder compacts after sintering at 1650 °C. (a) 90 Al_2O_3–10 ZrO_2; (b) 87.5 Al_2O_3–12.5 ZrO_2; (c) 85 Al_2O_3–15 ZrO_2; (d) 80 Al_2O_3–20 ZrO_2; A, α-Al_2O_3; T, t-ZrO_2; M, m-ZrO_2.

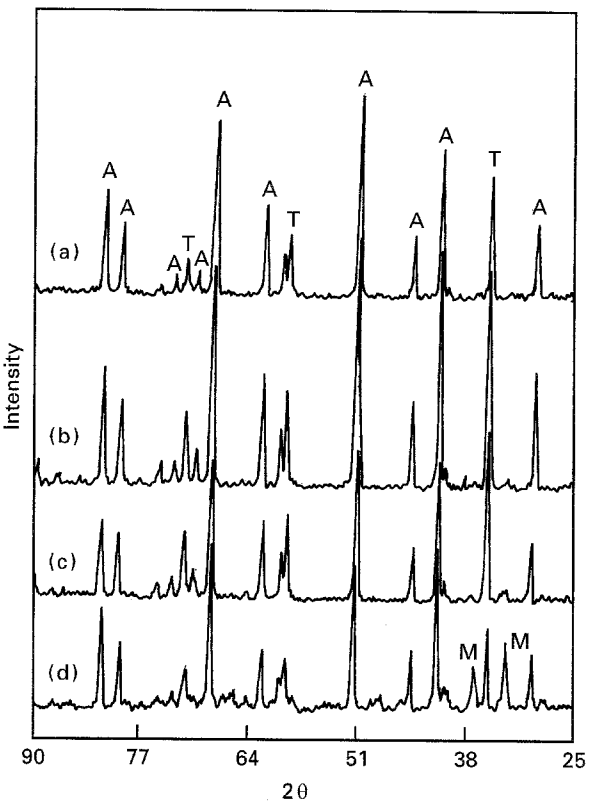

Figure 8 XRD patterns of the CAL9 powder compacts after sintering at 1650 °C. (a) 90 Al_2O_3–10 ZrO_2; (b) 87.5 Al_2O_3–12.5 ZrO_2; (c) 85 Al_2O_3–15 ZrO_2; (d) 80 Al_2O_3–20 ZrO_2; A, α-Al_2O_3; T, t-ZrO_2; M, m-ZrO_2

TABLE II Density and weight loss of compacts after sintering at 1650 °C for 3 h

Composition	Powder calcined at 650 °C			Powder calcined at 950 °C		
	Green density (% ρ_t)	Sintered density (% ρ_t)	Weight loss after sintering (%)	Green density (% ρ_t)	Sintered density (% ρ_t)	Weight loss after sintering (%)
10.0% ZrO_2	35	73	31.34	42	88	5.18
12.5% ZrO_2	37	66	28.77	41	90	4.14
15.0% ZrO_2	36	74	26.43	40	89	4.51
20.0% ZrO_2	33	66	22.36	41	87	4.28

is a minor phase.) This is well below the critical size to retain the tetragonal form [9].

Since the CAL6 powders were containing higher amount of hydrates, some amount of energy is utilized for the evolution of hydrates (an endothermic process), during sintering of the compacts and thus a lesser amount of energy is available for sintering. Also the escaped hydrates will generate pores. It is well established that pores trapped within α grains during the final stage of conventional sintering of α-Al_2O_3 are extremely difficult to remove [26]. These two factors are responsible for the low sintered density.

For the lower ZrO_2 contents the ZrO_2 grain size always lies below the critical diameter. In a previous study [9] it was reported that when the ZrO_2 content is higher than 10 vol % (~ 15 wt %) the ZrO_2 grain size increases, and a part of the ZrO_2 is transformed into the monoclinic phase during cooling. In this study tetragonal form is retained almost fully for the CAL6 powder derived compacts. In the case of CAL9 derived compacts, nearly 100% t-ZrO_2 is retained up to compositions containing 15 wt % ZrO_2 whereas more than half of t-ZrO_2 is transformed when the ZrO_2 content is 20 wt %. Murase *et al.* [13] found that the crystallite growth of ZrO_2 was negligible in the presence of Al_2O_3 whereas a remarkable increase was observed in the pure ZrO_2 powders. An increasing amount of t-ZrO_2 was present as the Al_2O_3 content increases. It was suggested that this might be the effect of stresses applied to ZrO_2 particles interposed among the Al_2O_3 particles which have been tightly bonded at high temperatures [13]. The critical size needed to stabilize the tetragonal form is lower for higher ZrO_2 content [9]. Becher [27] considered that there was a critical volume fraction of a given particle size to cause the transformation. It is based on the fact that an internal tensile stress is produced due to the thermal expansion mismatch of Al_2O_3 ($\alpha = 8.1 \times 10^{-6} K^{-1}$) and ZrO_2 ($\alpha = 10.5 \times 10^{-6} K^{-1}$). This internal tensile stress increases with increasing

amount of ZrO_2. When the ZrO_2 content is above a critical level, the tensile stress is equal to the stress required for transformation. Thus the ZrO_2 grain growth and the internal tensile stress are responsible for the tetragonal to monoclinic transformation in the CAL9 samples containing 20 wt % ZrO_2. Higher amount of t-ZrO_2 retained in the CAL6 samples containing 20 wt % ZrO_2 is probably due to the smaller ZrO_2 grains. The smaller grain size results from the inhibition of growth by the higher amount of pores present in the sample [28].

5. Conclusions

Al_2O_3–ZrO_2 composite powders of average particle size 6 μm were prepared by spray drying. The initial amorphous powders are crystallized to t-ZrO_2, δ-Al_2O_3 and α-Al_2O_3 after calcining at 950 °C. Calcination also modifies the surface structure of particles. For a better sintered density, the calcination at 950 °C is preferable. Retention of nearly 100% t-ZrO_2 without the stabilizing oxides is possible in the dense composites containing up to 15 wt % ZrO_2.

References

1. A. G. EVANS and R. M. CANNON, *Acta. Metall.* **34** (1986) 761.
2. M. RUHLE, N. CLAUSSEN and A. H. HEUER, *J. Amer. Ceram. Soc.* **69** (1986) 195.
3. N. L. HECHT, S. M. GOODRICH, D. E. McCULLUM, P. P. YANEY, S. D. JUNG and V. J. TENNERY, *Amer. Ceram. Soc. Bull.* **71** (1992) 955.
4. J. WANG and R. STEVENS, *J. Mater. Sci.* **24** (1989) 3421.
5. F. F. LANGE, *ibid.* **17** (1982) 225.
6. A. H. HEUER, N. CLAUSSEN, W. M. KRIVEN and M. RUHLE, *J. Amer. Ceram. Soc.* **65** (1982) 642.
7. R. C. GARVIE, *J. Phys. Chem.* **69** (1965) 1238.
8. *Idem., ibid.* **82** (1978) 218.
9. J. P. BACH and F. THEVENOT, *J. Mater. Sci.* **24** (1989) 2711.
10. S. DICK, C. SUHR, J. L. REHSPRINGER and M. DAIRE, *Mater. Sci. Eng. A* **109** (1989) 227.
11. H. YOSHIMATSU, T. YABUKI and H. KAWASAKI, *J. Non-Cryst. Solids* **100** (1988) 413.
12. W. D. BOND and P. F. BECHER, in "Ultrastructure processing of advanced ceramics", edited by J. D. Mackenzie and D. R. Ulrich (Wiley, New York, 1988) p. 443.
13. Y. MURASE, E. KATO and K. DAIMON, *J. Amer. Ceram. Soc.* **69** (1986) 83.
14. C. S. HWANG and S. C. TSAUR, *J. Mater., Sci.* **27** (1992) 6791.
15. F. F. LANGE, *ibid.* **17** (1982) 247.
16. A. G. EVANS, N. BURLINGAME, M. DRORY and W. M. KRIVEN, *Acta. Metall.* **29** (1981) 447.
17. L. MONTANARO and A. NEGRO, *J. Mater. Sci.* **26** (1991) 4511.
18. R. C. GARVIE and P. S. NICHOLSON, *J. Amer. Ceram. Soc.* **55** (1972) 303.
19. T. SATO, S. IKOMA and F. OZAWA, in "Thermal analysis" edited by B. Miller (John Wiley & Sons, Chichester, 1982) p. 578.
20. V. SARASWATI, G. V. N. RAO and G. V. RAMA RAO, *J. Mater. Sci.* **22** (1987) 2529.
21. H. A. SZYMANSKI, in "Infrared band handbook" (Plenum Press, New York, 1963) p. 198, 207.
22. J. PERI, *J. Phys. Chem.* **69** (1965) 211.
23. B. G. LINSEN, in "Physical and chemical aspects of adsorbents and catalysts" (Academic Press, London, 1970) p. 195.
24. R. CYPRES, R. WOLLAST and J. RAUEQ, *Ber. Deut. Keram. Ges.* **40** (1963) 527.
25. P. VINCENZINI, in "Fundamentals of ceramic engineering" (Elsevier Applied Science, London, 1991) p. 133.
26. J. E. BURKE, *J. Amer. Ceram. Soc.* **40** (1957) 80.
27. P. F. BECHER, *Acta Metall.* **34** (1986) 1885.
28. F. F. LANGE, *J. Amer. Ceram. Soc.* **67** (1984) 83.

Received 15 December 1993
and accepted 4 November 1994